

CM-MaskSD: Cross-Modality Masked Self-Distillation for Referring Image Segmentation

Wenxuan Wang*

s20200579@xs.ustb.edu.cn

School of Automation and Electrical Engineering, University of Science and Technology Beijing
Beijing, China

Jing Liu

jliu@nlpr.ia.ac.cn

National Laboratory of Pattern Recognition, Institute of Automation, Chinese Academy of Sciences; University of Chinese Academy of Sciences
Beijing, China

Xingjian He

xingjian.he@nlpr.ia.ac.cn

National Laboratory of Pattern Recognition, Institute of Automation, Chinese Academy of Sciences; University of Chinese Academy of Sciences
Beijing, China

Yisi Zhang

School of Automation and Electrical Engineering, University of Science and Technology Beijing
Beijing, China

Chen Chen

chen.chen@crcv.ucf.edu

Center for Research in Computer Vision, University of Central Florida
Orlando, United States

Jiachen Shen

School of Automation and Electrical Engineering, University of Science and Technology Beijing
Beijing, China

Yan Zhang

School of Automation and Electrical Engineering, University of Science and Technology Beijing
Beijing, China

Jiangyun Li[†]

leejy@ustb.edu.cn

School of Automation and Electrical Engineering, University of Science and Technology Beijing
Beijing, China

ABSTRACT

Referring image segmentation (RIS) is a fundamental vision-language task that intends to segment a desired object from an image based on a given natural language expression. Due to the essentially distinct data properties between image and text, most of existing methods either introduce complex designs towards fine-grained vision-language alignment or lack required dense alignment, resulting in scalability issues or mis-segmentation problems such as over- or under-segmentation. To achieve effective and efficient fine-grained feature alignment in the RIS task, we explore the potential of masked multimodal modeling coupled with self-distillation and propose a novel cross-modality masked self-distillation framework named CM-MaskSD, in which our method inherits the transferred knowledge of image-text semantic alignment from CLIP model to realize fine-grained patch-word feature alignment for better segmentation accuracy. Moreover, our CM-MaskSD framework can considerably boost model performance in a nearly parameter-free manner, since it shares weights between the main segmentation branch and the introduced masked self-distillation branches, and solely introduces negligible parameters for coordinating the multi-modal features. Comprehensive experiments on three benchmark datasets (*i.e.* RefCOCO, RefCOCO+, G-Ref) for the RIS task convincingly demonstrate the superiority of our proposed framework over previous state-of-the-art methods.

CCS CONCEPTS

• **Computing methodologies** → **Image segmentation.**

KEYWORDS

Referring Image Segmentation, Cross-Modality Guidance, Masked Self-Distillation, Vision and Language

1 INTRODUCTION

Referring image segmentation (RIS) aims to segment specific regions of input images corresponding to the given language expression. RIS has become one of the most challenging vision-language tasks due to its requirement for mutual understanding across the two different modalities. In addition, compared with conventional single-modality (*i.e.* image or video) segmentation, RIS partly resolves the limitations of segmentation targets solely on predefined categories. Considering that diverse targets are required in real-world downstream tasks, RIS could potentially be employed in a wide range of applications, including language-based human-object interaction and interactive image editing.

Since the concept of RIS task was initially proposed in [10], different multimodal frameworks for referring image segmentation have been designed to deal with the feature extraction and interaction between visual and linguistic modalities, including the first attempt of introducing recurrent LSTM network [10], CLIP-driven framework [38], language-aware vision Transformer network [42], and convolution-free network [18]. However, due to the considerable

*This work was performed while Wenxuan worked as an intern at National Laboratory of Pattern Recognition, Institute of Automation, Chinese Academy of Sciences.

[†]Corresponding Author

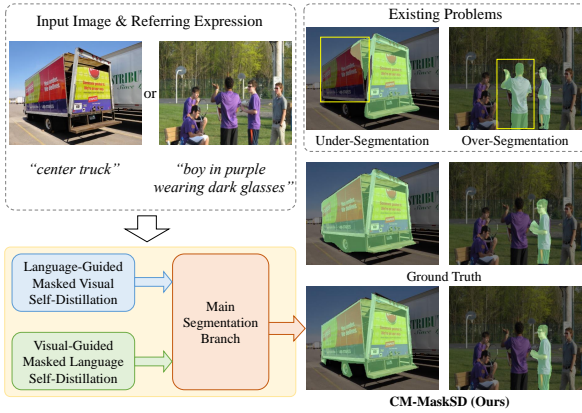


Figure 1: The illustration of our CM-MaskSD pipeline for referring image segmentation.

differences between visual and language modalities, feature alignment has become a crucial challenge for precise segmentation. Previous works have made great efforts to overcome this challenge. For instance, CRIS [38] achieves semantic consistency by propagating semantic information from textual representations to each image pixel, yet it neglects to correlate the important visual information with language representations. LAVT [42] enhances the model’s capability of cross-modality alignment through a multi-stage structure, yet such a sophisticated network is inflexible for further improving fine-grained feature alignment. It is notable that without aligning cross-modality information correctly, models are prone to the mis-segmentation problem (*i.e.* over- and under-segmentation). As shown in Fig. 1, models could not generate a complete segmentation mask of the main parts without adequate exploration of the correlation between image regions and their relevant words, leading to the under-segmentation problem. Besides, image regions with essentially weak relevance to the whole expression may be wrongly guided by some misleading words in the given text, resulting in the over-segmentation problem. As shown in the second column on the right side of Fig. 1, rather than generating the segmentation mask of the specific boy wearing dark glasses, CRIS [38] has segmented redundant parts (*i.e.* another boy in purple without wearing glasses) since the less important words (boy in purple) are wrongly considered as the most relevant with the image. Although advanced models could be adopted for comprehensive feature extraction of the given images and texts, a novel generic framework is expected to overcome the aforementioned two drawbacks and effectively realize more fine-grained feature alignment.

Therefore, to better assist models in mastering the capability of fine-grained feature alignment, we explore the potential of masked self-distillation applying to referring image segmentation task for the first time. In this paper, we provide a **Cross-Modality Masked Self-Distillation** framework (CM-MaskSD) to densely correlate the multimodal features in a simple and efficient manner. As shown in Fig. 1, our proposed framework enables effective mutual guidance between visual and textual modalities by taking advantage of the bidirectional cross-modality interaction. Except for the main branch for realizing the segmentation task, two symmetric branches are additionally designed for masked self-distillation. The first branch is the language-guided masked visual self-distillation branch, in

which we introduce the textual global features from the language encoder to guide the masked visual self-distillation. Specifically, the correlation vector is firstly calculated between the visual feature embeddings of image patches and the textual global token, then the TopK text-related image patches that are most related to textual global representations are selected. We randomly mask the embedded features of TopK related image patches with a masking ratio α and send all the resulted visual tokens into the following model for segmentation. To implicitly guide model to achieve dense alignment between visual and textual features, the optimization target is conducted by pulling closer the segmentation results of masked visual self-distillation branch and the main segmentation branch (*i.e.* without any masking). Similarly, the visual-guided masked language self-distillation branch is symmetric to the aforementioned masked visual self-distillation branch. Finally, by jointly employing the bilateral masked self-distillation branches, our framework could realize more fine-grained multimodal feature alignment, hence accomplishing the referring image segmentation task in a more precise manner. Noticeably, based on the main segmentation branch (*i.e.* a strong baseline), our masked self-distillation design solely introduces negligible parameters yet can greatly boost model performance via sharing weights between the self-distillation branches and the main branch. The experimental results clearly show that our proposed framework achieves superior performance over previous state-of-the-art (SOTA) approaches on the three benchmark datasets for the RIS task.

Our main contributions can be summarized as follows:

- We present the first study to explore the powerful potential of masked multimodal modeling with self-distillation for RIS task. The proposed CM-MaskSD framework can inherit the transferred knowledge of image-text semantic alignment from CLIP model to realize the dense text-patch feature alignment for higher segmentation accuracy.
- By fully taking advantage of the proposed cross-modality guided masked self-distillation and correlation filtering, our method can both efficiently and effectively achieve more fine-grained multimodal vision-language feature alignment, which is crucial for the RIS task.
- The proposed CM-MaskSD is a simple yet effective and generic framework that can be integrated with different ViT-based architectures, among which our masked self-distillation design is essentially plug-and-play and easy-to-implement.
- The experimental results on three benchmark datasets for referring image segmentation convincingly demonstrate the superiority of our CM-MaskSD over previous state-of-the-art methods. Moreover, via sharing weights, our framework can consistently boost model performance in a nearly parameter-free manner.

2 RELATED WORK

Referring Image Segmentation is to generate the category masks of target objects in an image according to the given natural language description. Since the input consists of multimodal information, constructing an effective framework for feature modeling and interaction between textual and visual features is considered the most crucial part of the entire task. The RIS task is first brought up in [10], which simply concatenates linguistic and visual features

extracted by LSTM [9] and convolutional neural network separately, and predicts the final segmentation mask through a fully connected network. Some of the subsequent works [34] [29] [21] follow the paradigm of modeling text expression and image features independently, and then set fusion pipeline to introduce language information into pixel-level activation. However, [23] believes that joint modeling is more intrinsic for RIS task and proposes the multimodal ConvLSTM to encode visual information, spatial cues and the sequential interaction between each word. Nevertheless, rather than regarding the input sentence as an individual unit, MattNet [44] treats it as a hybrid of objects' position, appearance and relationship to others, putting forward a two-stage network to select generated regions of interest with textual guidance. Different from the aforementioned methods that employ implicit feature interaction and fusion between visual and linguistic modalities, [13] tends to adopt a progressive manner, using entity and attribute words to perceive all the entities involved in the expression and further inferring the relationship between entities to highlight the relevant objects of referring expression. Besides, motivated by previous application of contrastive learning in language-image pre-training, CRIS [38] propagates fine-grained semantic information from text to visual embeddings via a joint visual-language decoder and enhances cross-modality consistency with contrastive learning.

As Transformer and attention mechanisms have been well studied in various linguistic and visual downstream tasks, their advantage over convolutional neural networks in capturing long-range dependency seems apparent. In CMSA [43], cross-modality self-attention module is employed to obtain long-range dependency between two modalities. VLT [5] redefines RIS as a direct attention problem, introducing Transformer and multi-head attention to query a given image with the language expression. ReSTR [18] is proposed as the first convolution-free, Transformer-based referring image segmentation model, which only uses different Transformer encoders to realize the respective feature extraction of text and image and the following multiple interactions between them. Furthermore, LAVT [42] operates early multimodal feature fusion on the constructed multi-level Transformer encoder, achieving significantly better cross-modality alignment. In addition, [39] considers negative sentences as inputs to enhance the robustness of model to the misdescription or misleading by the given text.

Mask Image/Language Modeling is an effective self-supervised pre-training pattern for learning general representations, which has been studied in the field of natural language processing (NLP) and computer vision (CV). BERT [4] and its variants [25] [3] yield SOTA performance in a broad range of NLP tasks by introducing masked language modeling (MLM). With the success of MLM in the NLP field and the emergence of vision Transformers [6], BEiT [2] and BEiTV2 [32] introduce a classifier to predict masked image tokens, which is supervised by the encoded visual patches from offline tokenizer. SimMIM [40] directly adopts the low-level image features (*i.e.* pixel's RGB value) as prediction targets, leading to considerable performance gains compared to conventional self-supervised pretext tasks (*e.g.* patch classification). Instead of feeding masked tokens as input to the encoder, MAE [8] develops a straightforward decoder to reconstruct image patches, resulting in a significant decrease in pre-training computational costs. To break the limitation that MAE-based methods can only be performed on

the standard vision Transformers [6], a lot of works [12, 24, 36] have been proposed.

As a powerful model compression technique, self-knowledge distillation has also shown impressive performance in masked image modeling. In order to improve the model training efficiency, DMJD [28] adheres to the training scheme of disjoint masking and joint distillation. Instead of directly imitating the output of teacher network, MGD [41] allows the student model to recover teacher model's feature representations with randomly masked feature maps, achieving excellent improvements on various visual downstream tasks. Similarly, DMAE [1] aligns the intermediate features between teacher model and student model, studying the potential of distilling knowledge from MAE. However, considering that not all pixels of feature maps contribute equally to model performance, MaskKD [14] utilizes masked feature distillation to prompt student model to adaptively learn the values of the teacher model's feature maps at each position based on their informative contribution. Such an attention-aware idea can also be directly applied to the masking process. For instance, MaskedKD [35] leverages the attention maps learned by student model to mask the input image of teacher network, providing a simple yet efficient strategy to reduce the distillation cost of ViT.

Different from the above works, in this paper, we conduct the pioneering exploration on building an effective and also efficient masked self-distillation architecture on both text and image modalities for better accomplishing RIS task. Specifically, two symmetric distillation branches are designed to enhance the model's comprehension of mutual correlations between the feature representations of language expression and image. Among each branch, cross-modality guided correlation filtering and the following masking operation are performed to promote the expected fine-grained feature alignment.

3 METHODOLOGY

As shown in Fig. 2, our Cross-Modality Masked Self-Distillation (CM-MaskSD) framework includes a multi-modal main segmentation branch and two symmetric masked self-distillation branches that are designed for achieving more fine-grained feature alignment between referring expression and visual representations. The details of our CM-MaskSD are presented in the following.

3.1 Main Segmentation Branch

Since CLIP [33] is capable of directly learning transferable visual concepts from large-scale collections of image-text pairs, we leverage the pre-trained weights of CLIP as our segmentation backbone. To obtain the extracted visual and linguistic feature representations, the image encoder and the text encoder are employed respectively. Given the input image I and referring text T , we first send them to the feature embedding layer to obtain the visual embedding E_I and textual embedding E_T . These embedded feature tokens are then fed to their respective encoders to obtain the visual and textual feature representations, which can be expressed as follows:

$$\begin{aligned} V_{local}, v_{global} &= \text{CLIP Image Encoder}(E_I) \\ W_{local}, w_{global} &= \text{CLIP Text Encoder}(E_T) \end{aligned} \quad (1)$$

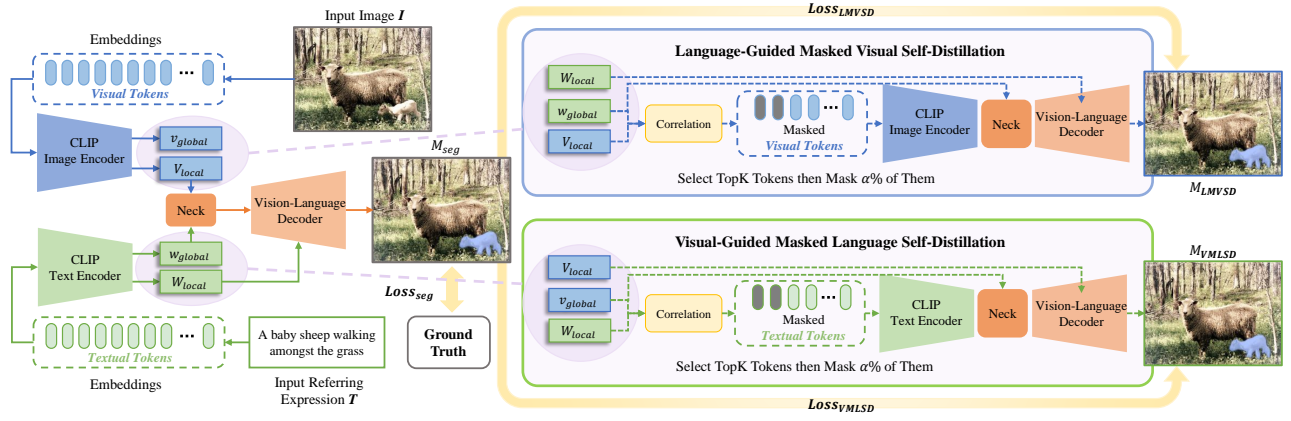


Figure 2: The architecture of our CM-MaskSD framework. It consists of a multimodal segmentation branch and two symmetric masked self-distillation branches that are designed for more fine-grained visual and textual feature alignment. During training, the main segmentation loss $Loss_{seg}$ coupled with two self-distillation loss $Loss_{LMVSD}$ and $Loss_{VMLSD}$ are jointly employed to pull close the segmentation masks generated by the main branch and the cross-modality guided masked self-distillation branches. For inference, only the main segmentation branch is preserved to acquire the final segmentation masks.

where V_{local} and W_{local} are the output sequences of visual and textual tokens respectively, each of which corresponds to a single visual image patch or a textual word. v_{global} denotes the [class] token that serves as the image-level representation with strong semantics. w_{global} is the text-level representation which is the aggregated feature representation of all textual tokens W_{local} . Subsequently, an effective neck module is used to fuse the multimodal feature F by taking V_{local} and w_{global} as input, followed by a vision-language decoder that generates the final segmentation results M_{seg} . Note that the employed neck and vision-language decoder are solely introduced to provide a strong segmentation baseline, which follows the same standard architecture as CRIS [38].

$$\begin{aligned} F &= \text{Neck}(V_{local}, w_{global}) \\ M_{seg} &= \text{Vision-Language Decoder}(F, W_{local}) \end{aligned} \quad (2)$$

3.2 Cross-Modality Masked Self-Distillation

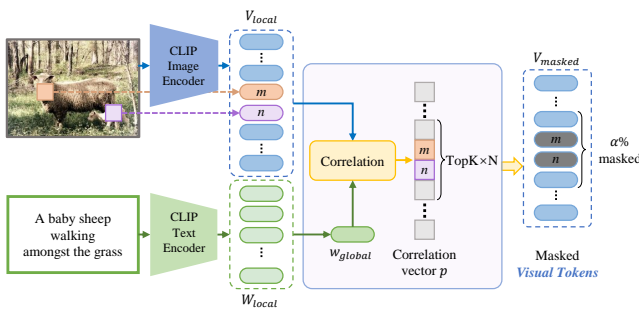


Figure 3: The illustration of the introduced correlation filtering and cross-modality guided masking strategy in our language-guided masked visual self-distillation branch.

Although employing the CLIP model [33] as backbone can inherit powerful image-level visual concepts from large-scale pre-training, this form of knowledge is insufficient for referring image

segmentation owing to the absence of fine-grained cross-modality feature alignment. To better solve this issue, we propose the CM-MaskSD framework to implicitly realize dense alignment between word-level textual representations and pixel-level visual features.

Language-Guided Masked Visual Self-Distillation (LMVSD). Based on the obtained visual and linguistic features in Sec. 3.1, we utilize the text-level representation $w_{global} \in \mathbb{R}^{1 \times C}$ and $V_{local} = (v_0, v_1, \dots, v_{N-1}) \in \mathbb{R}^{N \times C}$, where $v_i \in \mathbb{R}^{1 \times C}$, we calculate the correlation vector p between them. Next, the T visual feature tokens among V_{local} that have the highest correlation values in the correlation vector p will be selected.

$$\begin{aligned} p_i &= w_{global} \cdot v_i, \text{ where } i = 0, 1, \dots, N-1 \\ p &= (p_0, p_1, \dots, p_j, p_{j+1}, \dots, p_{j+T-1}, p_{j+T}, \dots, p_{N-1}) \quad (3) \\ &\quad T, 0 \leq j, T \leq N \end{aligned}$$

where \cdot denotes the dot product operation, $T = \text{TopK} \times N$, N denotes the number of selected visual tokens after correlation filtering.

As shown in Fig. 3, these T visual tokens can be categorized into two groups: (1) feature tokens that do not match the expectation (i.e. the specific visual tokens are essentially not correlated with the current text), which may mislead the entire model and further induce over-segmentation (e.g. visual tokens of the adult sheep, as the m_{th} visual token highlighted with orange color in Fig. 3) and (2) feature tokens that match our expectations (i.e. the specific visual tokens are strongly correlated with the current text in essence) and correlate densely with the given expression (e.g. visual tokens of the baby sheep, as the n_{th} visual token highlighted with purple color in Fig. 3), which directly contributes to the model's segmentation accuracy. Then we randomly mask the selected T feature tokens according to a suitable masking ratio $\alpha\%$, which involves replacing them with randomly initialized learnable tokens v' .

$$V_{masked} = (v_0, v_1, \dots, \underbrace{v', v', \dots, v'}_{\alpha\% \times T}, \dots, v_{N-1}) \quad (4)$$

When the first type of visual tokens are masked, we apply a self-distillation loss $Loss_{LMVSD}$ to ensure that the corresponding segmentation result M_{LMVSD} is consistent with the output prediction of main segmentation branch. In this way, the model can associate the accurate fine-grained visual-textual features more closely and at the same time draw a clear line between the visual-textual features that should not produce strong associations. Therefore, the model will not be misguided by other misleading textual information, greatly avoiding the model from over-segmentation. Simultaneously, when the second type of visual feature tokens are masked, we also use $Loss_{LMVSD}$ to ensure that the segmentation result M_{LMVSD} of this branch is consistent with the output prediction of main segmentation branch. Since masking the corresponding tokens makes it harder for the visual distillation branch to predict segmentation result that is consistent with the main branch, this design can essentially guide the model to generate more complete segmentation masks, implicitly preventing the model from under-segmentation. With this language-guided masked visual self-distillation branch, the model can realize a more fine-grained alignment between the textual global features and the visual tokens than before.

To predict the segmentation results M_{LMVSD} , we feed the masked visual tokens V_{masked} into the combination of the CLIP image encoder, neck and vision-language decoder, which stays the same architecture as the main segmentation branch. To be noticed, the parameters of all these three components are shared with the main segmentation branch to pursue a parameter-efficient architecture.

$$\begin{aligned} V'_{local}, v'_{global} &= \text{CLIP Image Encoder}(V_{masked}) \\ F_{LMVSD} &= \text{Neck}(V'_{local}, w_{global}) \\ M_{LMVSD} &= \text{Vision-Language Decoder}(F_{LMVSD}, W_{local}) \end{aligned} \quad (5)$$

Visual-Guided Masked Language Self-Distillation (VMLSD). Symmetric to LMVSD elaborated above, the acquired global visual feature v_{global} is utilized to guide the masked language self-distillation process in our proposed VMLSD. Given $v_{global} \in \mathbb{R}^{1 \times C}$ and $W_{local} = (w_0, w_1, \dots, w_{N-1})$, where $w_i \in \mathbb{R}^{1 \times C}$, $W_{local} \in \mathbb{R}^{N \times C}$, we calculate the correlation vector q between v_{global} and each w_i , which measures the image-word similarity.

$$\begin{aligned} q_i &= v_{global} \cdot w_i, \text{ where } i = 0, 1, \dots, N-1 \\ q &= (q_0, q_1, \dots, \underbrace{q_j, q_{j+1}, \dots, q_{j+T-1}}_{T, 0 \leq j, T \leq N}, q_{j+T}, \dots, q_{N-1}) \end{aligned} \quad (6)$$

where $T = TopK \times N$. Then, the T textual tokens in W_{local} that have the highest correlation values in q are selected, and $\alpha\%$ of them are randomly masked by randomly initialized learnable tokens w' which have the same shape as w_i .

$$W_{masked} = (w_0, w_1, \dots, \underbrace{w', w', \dots, w'}_{\alpha\% \times T}, \dots, w_{N-1}) \quad (7)$$

Through this process, the masked textual tokens W_{masked} are obtained and fed into the combination of the CLIP text encoder, neck and vision-language decoder that stays the same architecture as main segmentation branch, to predict the segmentation results M_{VMLSD} . Similarly, the parameters of the CLIP text encoder, neck and vision-language decoder in VMLSD branch are all shared with

the main branch to ensure the model efficiency. Benefiting from this visual-guided masked language self-distillation branch, the whole network can realize a more fine-grained alignment between the visual global features and the textual word tokens than previous.

$$\begin{aligned} W'_{local}, w'_{global} &= \text{CLIP Image Encoder}(W_{masked}) \\ F_{VMLSD} &= \text{Neck}(W'_{local}, v_{global}) \\ M_{VMLSD} &= \text{Vision-Language Decoder}(F_{VMLSD}, V_{local}) \end{aligned} \quad (8)$$

3.3 Network Optimization

During the training phase, a compound loss function $Loss_{total}$ is adopted to constrain our model to align the word-level representations with the relevant pixel-level visual features. The compound loss consists of three components: (1) $Loss_{seg}$, which following CRIS [38] is a binary cross entropy (BCE) loss used to optimize the main segmentation branch and ensure accurate segmentation results; (2) $Loss_{LMVSD}$, a binary cross entropy loss, which constrains the consistency between the output of the LMVSD branch and the segmentation results output by the main segmentation branch M_{seg} ; (3) $Loss_{VMLSD}$, similar to $Loss_{LMVSD}$, which constrains the consistency between the output of the VMLSD branch and the final segmentation results M_{seg} . $Loss_{LMVSD}$ and $Loss_{VMLSD}$ jointly ensure a more dense alignment between the referring expression words and image patches, implicitly preventing the whole model from over-segmentation and under-segmentation. The total loss is defined as follows:

$$\begin{aligned} Loss_{seg} &= \text{BCELoss}(M_{seg}, GT) \\ Loss_{LMVSD} &= \text{BCELoss}(M_{LMVSD}, M_{seg}) \\ Loss_{VMLSD} &= \text{BCELoss}(M_{VMLSD}, M_{seg}) \\ Loss_{total} &= Loss_{seg} + \lambda_1 Loss_{LMVSD} + \lambda_2 Loss_{VMLSD} \end{aligned} \quad (9)$$

Here, GT denotes the Ground Truth. λ_1 and λ_2 are hyper-parameters that control the relative importance of the two self-distillation losses. By optimizing this joint loss $Loss_{total}$, our model can learn to generate more accurate and fine-grained segmentation results that are precisely aligned with the referring expressions. To be noticed, during the inference phase, only the main segmentation branch is reserved to obtain the corresponding segmentation masks.

4 EXPERIMENTAL RESULTS

To evaluate the effectiveness and the designing rationale of our method, comprehensive experiments are conducted on three benchmark datasets, including RefCOCO, RefCOCO+ and G-Ref.

4.1 Datasets

RefCOCO [45] is one of the largest and most commonly used datasets collected from the MSCOCO [22] for referring image segmentation task, which includes 142,209 annotated expressions (average length of 3.6 words) for 50,000 objects in 19,994 images. The RefCOCO dataset is split into training, validation, test A, and test B with 120,624, 10,834, 5,657 and 5,095 samples respectively.

RefCOCO+ [17] dataset contains 141,564 language expressions (average length of 3.5 words) with 49,856 objects in 19,992 images, which is separately split into training, validation, test A, and test B with 120,624, 10,758, 5,726, and 4,889 samples. Compared to RefCOCO, some language expressions with absolute location

Table 1: Comparisons with the state-of-the-art approaches on three referring image segmentation benchmark datasets. “★” denotes the post-processing of DenseCRF [19]. “-” denotes that the result is not provided. The evaluation metric is IoU.

Method	Vision Backbone	Language Encoder	RefCOCO			RefCOCO+			G-Ref	
			val	test A	test B	val	test A	test B	val	test
RMI★ [23]	ResNet-101	LSTM	45.18	45.69	45.57	29.86	30.48	29.50	-	-
DMN [29]	ResNet-101	SRU	49.78	54.83	45.13	38.88	44.22	32.29	-	-
RRN★ [21]	ResNet-101	LSTM	55.33	57.26	53.95	39.75	42.15	36.11	-	-
MAttNet [44]	ResNet-101	Bi-LSTM	56.51	62.37	51.70	46.67	52.39	40.08	47.64	48.61
CMSA★ [43]	ResNet-101	None	58.32	60.61	55.09	43.76	47.60	37.89	-	-
BCAN★ [11]	ResNet-101	LSTM	61.35	63.37	59.57	48.57	52.87	42.13	-	-
CMPC★ [13]	ResNet-101	LSTM	61.36	64.53	59.64	49.56	53.44	43.23	-	-
LSCM★ [15]	ResNet-101	LSTM	61.47	64.99	59.55	49.34	53.12	43.50	-	-
MCN [27]	DarkNet-53	Bi-GRU	62.44	64.20	59.71	50.62	54.99	44.69	49.22	49.40
CGAN [26]	DarkNet-53	Bi-GRU	64.86	68.04	62.07	51.03	55.51	44.06	51.01	51.69
EFNet [7]	ResNet-101	Bi-GRU	62.76	65.69	59.67	51.50	55.24	43.01	-	-
LTS [16]	DarkNet-53	Bi-GRU	65.43	67.76	63.08	54.21	58.32	48.02	54.40	54.25
VLT [5]	DarkNet-53	Bi-GRU	65.65	68.29	62.73	55.50	59.20	49.36	52.99	56.65
ReSTR [18]	ViT-Base	Transformer	67.22	69.30	64.45	55.78	60.44	48.27	-	-
SeqTR [46]	DarkNet-53	Bi-GRU	67.26	69.79	64.12	54.14	58.93	48.19	55.67	55.64
CRIS [38]	CLIP-RN101	CLIP	70.47	73.18	66.10	62.27	68.08	53.68	59.87	60.36
RefTr [20]	ResNet-101	BERT-Base	70.56	73.49	66.57	61.08	64.69	52.73	58.73	58.51
LAVT [42]	Swin-Base	BERT-Base	72.73	75.82	68.79	62.14	68.38	55.10	61.24	62.09
CM-MaskSD (Ours)	CLIP-ViT-Base	CLIP	72.18	75.21	67.91	64.47	69.29	56.55	62.67	62.69
CM-MaskSD (Ours)	CLIP-ViT-Large	CLIP	74.89	77.54	71.28	67.47	71.80	59.91	66.53	66.63

descriptions are deleted in RefCOCO+ dataset, which makes it more challenging for RIS.

G-Ref [30], as the third benchmark dataset, includes 104,560 referring expressions (average length of 8.4 words) for 54,822 objects in 26,711 images. It collects the language expressions from Amazon Mechanical Turk, which is different from the former two datasets. Following previous work, the standard UMD partition [10] is adopted for evaluation in this paper.

4.2 Implementation Details

Experimental Setup. Our proposed framework is implemented based on Pytorch [31] and trained with Tesla V100 GPUs. Considering the crucial scalability and the ease of implementation, the Vision Transformer [6] is adopted as the image encoder for all the experiments. The text and image encoder are initialized by CLIP [33], while the rest part of model weights are randomly initialized. During training, the input images are resized to the resolution of 576×576 and 532×532 for ViT-Base and ViT-Large respectively for experimental comparisons with previous SOTA methods. To make an efficient and fair comparison, the resolution of 480×480 is adopted for ablation study. The Adam optimizer with 32 batch size and a weight decay of 0.0005 are adopted to train the model for 100 epochs. With a warm-up strategy for 10 epochs during training, the initial learning rate is set to 0.00001 with a cosine decay schedule. Following CRIS [38], due to the extra [SOS] and [EOS] tokens, the input sentences are set with a maximum sentence length of 17 for RefCOCO and RefCOCO+, 22 for G-Ref.

During inference, the predicted results by our method is upsampled back to the original image size and binarized with a threshold of 0.35 to the final segmentation result. Any extra post-processing

operations can be exploited to further boost the segmentation accuracy of our framework, but are not employed in this work.

Evaluation metrics. To evaluate our proposed method, we adopt mask Intersection-over-Union (IoU) and Precision@X as evaluation metrics. The IoU measures the ratio between the intersection area and the union area of the prediction and ground truth among the test samples. The Precision@X measures the percentage of test samples with an IoU score higher than the threshold X that ranges from 0.5 to 0.9 with an interval of 0.1. The Precision@X focuses on the location ability of different methods.

4.3 Main Results

Quantitative Analysis. To validate the superiority of our CM-MaskSD and make a fair comparison, our method is evaluated against the SOTA methods on RefCOCO [45], RefCOCO+ [17] and G-Ref [30] datasets. As presented in Table 1, our method outperforms the previous methods in terms of segmentation accuracy across all evaluation subsets of the three benchmark datasets. With ViT-Base [6] used as visual backbone and Transformer [37] as text encoder that are initialized by CLIP [33], our method obtains comparable or better performance compared with the latest SOTA method LAVT [42], especially showing dominant superiority on RefCOCO+ and G-Ref datasets. In comparison with CRIS [38] which also employs the CLIP model [42] as vision backbone and language encoder, significant performance improvement is achieved by our CM-MaskSD across all three benchmark datasets. Besides, to further explore the potential of our framework, ViT-Large initialized by CLIP [33] is further introduced as a stronger visual backbone. It can be clearly seen that the employment of ViT-Large as vision backbone enables our approach to further push the SOTA



Figure 4: The visual comparison of segmentation results on RefCOCO validation set. (a) the input image. (b) CRIS. (c) our proposed CM-MaskSD. (d) the ground truth.

results. Specifically, on RefCOCO dataset, our method achieves much higher SOTA results compared to LAVT, resulting in a significant margin of 2.16%, 1.72%, and 2.49% IoU on the validation, testA and testB sets respectively. On G-Ref dataset, our method surpasses the previous SOTA method LAVT [42] by a large gap (*i.e.* 5.29% and 4.54% IoU on the validation set and test set respectively). The same promising results can also be found on RefCOCO+ dataset. It is noteworthy that, instead of utilizing more powerful backbone (*e.g.* Swin Transformer) that is pre-trained through strongly supervised manner as feature extractor like LAVT [42], our CM-MaskSD solely takes advantage of the simple yet effective ViT structure pre-trained through unsupervised manner [33], not to mention that our method possesses strong scalability and doesn't contain any complex designs. Based on the above analysis, all the experimental results convincingly demonstrate that our CM-MaskSD framework can better accomplish the RIS task by pursuing finer-grained cross-modality feature alignment.

Qualitative Analysis. In addition, CRIS [38] and our proposed CM-MaskSD are further adopted for qualitative comparison since they both attempt to explore the powerful knowledge of CLIP model [33] for RIS task. The provided visualization results in Fig. 4 convincingly illustrate that our method can accomplish the RIS task more accurately and generate much better fine-grained segmentation masks of the corresponding objects, greatly reducing the segmentation errors caused by over-segmentation and under-segmentation.

4.4 Ablation Studies

We conduct extensive ablation experiments to justify the effectiveness of our design choice on RefCOCO validation set. ViT-Base initialized by CLIP is adopted for all the following ablation study.

Design of Masked Self-Distillation Manner. We first probe into the rationale of the proposed masked self-distillation design. As

Table 2: Ablation study on the design of masked self-distillation manner.

LMVSD	VMLSD	Pr@0.5	Pr@0.7	Pr@0.9	IoU
-	-	82.73	70.82	17.99	70.45
✓	-	83.90	73.54	20.08	71.45
-	✓	83.09	71.77	18.64	70.98
✓	✓	83.29	73.15	21.45	71.68

presented in Table 2, taking ViT-Base as the vision backbone, the baseline model obtains 70.45% IoU score on RefCOCO validation set. Either adding a single LMVSD branch or VMLSD branch to the whole architecture consistently leads to an considerable accuracy increase (1.00% and 0.53% IoU). Since the sequence length of visual tokens is much higher than the textual sequence and the RIS task is visually oriented in essence, the experimental results that masked visual self-distillation branch can bring higher performance improvements is clearly reasonable. In addition, by jointly employing both LMVSD and VMLSD branches in a nearly parameter-free manner, our method attains 1.23% improvements against the baseline. The above results fully demonstrate the benefit of exploiting the masked self-distillation framework for densely aligning linguistic and visual features. Besides, to show the advantage and designing rationale of our framework, we also present the visual comparison of the segmentation results in Fig. 5. It is clear that, compared with the baseline, our method can better solve the segmentation problem of under-segmentation and over-segmentation, benefiting from the introduced bilateral masked self-distillation branches.



Figure 5: Qualitative analysis for ablation study on our masked self-distillation design. (a) the input image. (b) baseline. (c) our proposed CM-MaskSD. (d) the ground truth.

Language-Guided Masked Visual Self-Distillation. Next, we explore the potential of our proposed LMVSD branch with different

Table 3: Ablation study on language-guided masked visual self-distillation.

Masking Ratio α (%)	TopK (%)	Loss Weight λ_1	Pr@0.5	Pr@0.7	Pr@0.9	IoU
(a) Loss weight λ_1						
0.25	0.5	0.1	83.20	71.88	19.40	70.93
0.25	0.5	0.25	83.73	73.03	19.74	71.36
0.25	0.5	0.5	83.51	72.61	19.13	71.17
0.25	0.5	0.75	83.90	73.54	20.08	71.45
0.25	0.5	1.0	82.63	72.53	20.79	70.72
(b) Mask ratio α(%)						
0.1	0.5	0.75	83.18	73.39	19.83	71.12
0.25	0.5	0.75	83.90	73.54	20.08	71.45
0.5	0.5	0.75	83.37	73.34	20.27	71.24
0.75	0.5	0.75	82.78	72.64	20.00	70.79
(c) TopK (%)						
0.25	0.25	0.75	83.21	73.41	20.61	71.09
0.25	0.5	0.75	83.90	73.54	20.08	71.45
0.25	0.75	0.75	82.88	73.13	19.68	70.93
0.25	1.0	0.75	83.08	73.13	20.77	71.01

hyper-parameter settings. Table 3 shows the ablation results of masking ratio α , TopK, and loss weight λ_1 of LMVSD branch. We sequentially explore the effects of these three hyper-parameters. Starting with loss weight λ_1 , five diverse settings (*i.e.* 0.1, 0.25, 0.5, 0.75, 1.0) are selected. It is clear that $\lambda_1 = 0.75$ enables the combination of baseline and our LMVSD branch to achieve the best performance. On this basis, lower λ_1 would result in inadequate self-distillation effect and would not take full advantage of the masked self-distillation design, while higher λ_1 leads to an adverse effect to the overall compound loss function during optimization process. Then we analyze the effect of different values of masking ratio α and TopK. Quantitative results in Table 3 show that with masking ratio set as 0.25 and TopK set as 0.5, the introduction of LMVSD branch leads to the best model performance. Higher masking ratio increases the difficulty of extracting visual features and generating the same segmentation masks as the main segmentation branch during self-distillation process, while lower masking ratio could cause certain information redundancy which hinders the whole structure from unleashing the power of masked self-distillation pipeline. Besides, if the TopK is set too high, our introduced correlation filtering may not effectively filter out relatively irrelevant visual tokens. On the contrary, if TopK is set too low, the range of the selected visual tokens after correlation filtering will be limited and much of the highly correlated visual tokens may be lost.

Visual-Guided Masked Language Self-Distillation. To further explore the potential of our proposed VMLSD branch, similar ablation study like LMVSD branch are conducted. Table 4 presents the experimental results. Different from the ablation study on LMVSD branch, the baseline with our VMLSD branch inserted obtains the best model performance when loss weight λ_2 , masking ratio α and TopK are set as 0.1, 0.1 and 0.5, respectively. Since the referring image segmentation is essentially a vision-dominated task, dislike the

Table 4: Ablation study on visual-guided masked language self-distillation.

Masking Ratio α (%)	TopK (%)	Loss Weight λ_2	Pr@0.5	Pr@0.7	Pr@0.9	IoU
(a) Loss weight λ_2						
0.1	0.5	0.05	82.76	71.78	18.73	70.58
0.1	0.5	0.1	83.09	71.77	18.64	70.98
0.1	0.5	0.25	83.02	71.40	18.69	70.41
0.1	0.5	0.5	82.34	70.86	18.52	70.02
0.1	0.5	0.75	81.12	69.92	18.17	69.47
0.1	0.5	1.0	81.07	70.25	17.76	69.28
(b) Mask ratio α(%)						
0.05	0.5	0.1	83.26	71.93	18.52	70.71
0.1	0.5	0.1	83.09	71.77	18.64	70.98
0.25	0.5	0.1	82.72	71.11	18.17	70.43
0.5	0.5	0.1	82.82	71.92	17.97	70.51
0.75	0.5	0.1	82.67	71.31	18.24	70.54
(c) TopK (%)						
0.1	0.25	0.1	83.22	72.12	18.18	70.68
0.1	0.5	0.1	83.09	71.77	18.64	70.98
0.1	0.75	0.1	82.66	71.09	18.07	70.23
0.1	1.0	0.1	82.92	71.66	18.32	70.57

Table 5: Ablation study on sharing weights for parameter-efficient masked self-distillation structure.

LMVSD	VMLSD	Sharing weights	Pr@0.5	Pr@0.7	Pr@0.9	IoU
-	-	-	82.73	70.82	17.99	70.45
✓	-	-	83.90	73.54	20.08	71.45
✓	-	✓	83.47	73.02	18.53	71.13
-	✓	-	83.09	71.77	18.64	70.98
-	✓	✓	83.29	71.80	18.28	70.88
✓	✓	-	83.26	72.24	19.03	71.26
✓	✓	✓	83.29	73.15	21.45	71.68

optimal setting $\lambda_1 = 0.75$ in the LMVSD branch, the VMLSD branch with $\lambda_2 = 0.1$ yields the best segmentation accuracy. Besides, since the visual-guided masking operation is performed at the word level, based on the textual low redundancy due to the short expression length (average 3.6 words on RefCOCO dataset), a high α will lead to the missing of important textual information. Additionally, similar to LMVSD branch, either the TopK is set unsuitably high or low, the segmentation accuracy would decrease, which is because the employed correlation filtering can not effectively filter out irrelevant textual information or much of the strongly correlated word tokens are accordingly lost for masked self-distillation.

Sharing Weights for Parameter-free Distillation Structure. Finally, we investigate the potential of our CM-MaskSD in the case of sharing weights for a parameter-efficient structure. The experimental results are presented in Table 5. Through sharing parameters of neck module and vision-language decoder between the

main branch and self-distillation branch, the introduction of either LMVSD branch or VMLSD branch leads to the performance improvement of 0.68% and 0.43% IoU respectively compared with the baseline. Although the resulted improvement is a little inferior to that without sharing parameters, employing the LMVSD branch or VMLSD branch in this parameter-efficient manner can consistently boost model performance with almost no additional parameters introduced. When both of the LMVSD branch and the VMLSD branch are simultaneously introduced, it leads to a 0.81% accuracy increase over the baseline under the circumstance of not sharing weights, which is not promising as the IoU score 71.45% made by solely introducing our LMVSD. We believe it is because that not sharing weights can not fully unleash the power of our cross-modality masked self-distillation structure due to the optimization difficulties, since all the parameters of these three branches (*i.e.* VMLSD branch, LMVSD branch and main segmentation branch) need to be optimized at the same time and there may be optimization collision between different parts. Thus, in order to effectively optimize the whole structure and to pursue a parameter-efficient framework, our CM-MaskSD adopts the designing scheme of sharing parameters and achieves the highest segmentation accuracy.

5 CONCLUSION AND FUTURE WORK

In this paper, we present the first study to explore the potential of masked multimodal modeling with self-distillation for RIS task and propose a novel framework CM-MaskSD that exploits masked multimodal modeling with self-distillation. It inherits transferred knowledge of image-text semantic alignment from CLIP and achieves dense feature alignment for improved segmentation accuracy. Our CM-MaskSD is scalable and flexible, integrating easily with ViT-based structures, among which our masked self-distillation design is essentially plug-and-play and easy-to-implement. Extensive experiments on three RIS benchmark datasets demonstrate that our CM-MaskSD greatly outperforms previous SOTA methods with negligible introduced parameters.

Our approach provides a novel solution to better guide the model to realize fine-grained feature alignment in RIS, inspiring new research in this direction. One potential limitation is that our framework mainly focus on ViT-based structures, but recent research suggests that our correlation filtering and cross-modality guided masking strategy can be accordingly adjusted to overcome this limitation. This provides a future research direction to develop a more general and powerful masked self-distillation framework that can assist various types of Transformer-based (*i.e.* hierarchical Swin Transformer) and CNN-based models in achieving dense multimodal feature alignment.

REFERENCES

- [1] Yutong Bai, Zeyu Wang, Junfei Xiao, Chen Wei, Huiyu Wang, Alan Yuille, Yuyin Zhou, and Cihang Xie. 2022. Masked autoencoders enable efficient knowledge distillers. *arXiv preprint arXiv:2208.12256* (2022).
- [2] Hangbo Bao, Li Dong, Songhao Piao, and Furu Wei. 2021. Beit: Bert pre-training of image transformers. *arXiv preprint arXiv:2106.08254* (2021).
- [3] Kevin Clark, Minh-Thang Luong, Quoc V Le, and Christopher D Manning. 2020. Electra: Pre-training text encoders as discriminators rather than generators. *arXiv preprint arXiv:2003.10555* (2020).
- [4] Jacob Devlin, Ming-Wei Chang, Kenton Lee, and Kristina Toutanova. 2018. Bert: Pre-training of deep bidirectional transformers for language understanding. *arXiv preprint arXiv:1810.04805* (2018).
- [5] Henghui Ding, Chang Liu, Suchen Wang, and Xudong Jiang. 2021. Vision-language transformer and query generation for referring segmentation. In *Proceedings of the IEEE/CVF International Conference on Computer Vision*. 16321–16330.
- [6] Alexey Dosovitskiy, Lucas Beyer, Alexander Kolesnikov, Dirk Weissenborn, Xiaohua Zhai, Thomas Unterthiner, Mostafa Dehghani, Matthias Minderer, Georg Heigold, Sylvain Gelly, et al. 2020. An image is worth 16x16 words: Transformers for image recognition at scale. *arXiv preprint arXiv:2010.11929* (2020).
- [7] Guang Feng, Zhiwei Hu, Lihe Zhang, and Huchuan Lu. 2021. Encoder fusion network with co-attention embedding for referring image segmentation. In *Proceedings of the IEEE/CVF Conference on Computer Vision and Pattern Recognition*. 15506–15515.
- [8] Kaiming He, Xinlei Chen, Saining Xie, Yanghao Li, Piotr Dollár, and Ross Girshick. 2022. Masked autoencoders are scalable vision learners. In *Proceedings of the IEEE/CVF Conference on Computer Vision and Pattern Recognition*. 16000–16009.
- [9] Sepp Hochreiter and Jürgen Schmidhuber. 1997. Long short-term memory. *Neural computation* 9, 8 (1997), 1735–1780.
- [10] Ronghang Hu, Marcus Rohrbach, and Trevor Darrell. 2016. Segmentation from natural language expressions. In *Computer Vision–ECCV 2016: 14th European Conference, Amsterdam, The Netherlands, October 11–14, 2016, Proceedings, Part I 14*. Springer, 108–124.
- [11] Zhiwei Hu, Guang Feng, Jiayu Sun, Lihe Zhang, and Huchuan Lu. 2020. Bi-directional relationship inferring network for referring image segmentation. In *Proceedings of the IEEE/CVF conference on computer vision and pattern recognition*. 4424–4433.
- [12] Lang Huang, Shan You, Mingkai Zheng, Fei Wang, Chen Qian, and Toshihiko Yamasaki. 2022. Green hierarchical vision transformer for masked image modeling. *arXiv preprint arXiv:2205.13515* (2022).
- [13] Shaofei Huang, Tianrui Hui, Si Liu, Guanbin Li, Yunchao Wei, Jizhong Han, Luoqi Liu, and Bo Li. 2020. Referring image segmentation via cross-modal progressive comprehension. In *Proceedings of the IEEE/CVF conference on computer vision and pattern recognition*. 10488–10497.
- [14] Tao Huang, Yuan Zhang, Shan You, Fei Wang, Chen Qian, Jian Cao, and Chang Xu. 2022. Masked Distillation with Receptive Tokens. *arXiv preprint arXiv:2205.14589* (2022).
- [15] Tianrui Hui, Si Liu, Shaofei Huang, Guanbin Li, Sansi Yu, Faxi Zhang, and Jizhong Han. 2020. Linguistic structure guided context modeling for referring image segmentation. In *Computer Vision–ECCV 2020: 16th European Conference, Glasgow, UK, August 23–28, 2020, Proceedings, Part X 16*. Springer, 59–75.
- [16] Ya Jing, Tao Kong, Wei Wang, Liang Wang, Lei Li, and Tieniu Tan. 2021. Locate then segment: A strong pipeline for referring image segmentation. In *Proceedings of the IEEE/CVF Conference on Computer Vision and Pattern Recognition*. 9858–9867.
- [17] Sahar Kazemzadeh, Vicente Ordonez, Mark Matten, and Tamara Berg. 2014. Referitgame: Referring to objects in photographs of natural scenes. In *Proceedings of the 2014 conference on empirical methods in natural language processing (EMNLP)*. 787–798.
- [18] Namyup Kim, Dongwon Kim, Cuiling Lan, Wenjun Zeng, and Suha Kwak. 2022. Restr: Convolution-free referring image segmentation using transformers. In *Proceedings of the IEEE/CVF Conference on Computer Vision and Pattern Recognition*. 18145–18154.
- [19] Philipp Krähenbühl and Vladlen Koltun. 2011. Efficient inference in fully connected crfs with gaussian edge potentials. *Advances in neural information processing systems* 24 (2011).
- [20] Muchen Li and Leonid Sigal. 2021. Referring transformer: A one-step approach to multi-task visual grounding. *Advances in neural information processing systems* 34 (2021), 19652–19664.
- [21] Ruiyu Li, Kaican Li, Yi-Chun Kuo, Michelle Shu, Xiaojuan Qi, Xiaoyong Shen, and Jiaya Jia. 2018. Referring image segmentation via recurrent refinement networks. In *Proceedings of the IEEE Conference on Computer Vision and Pattern Recognition*. 5745–5753.
- [22] Tsung-Yi Lin, Michael Maire, Serge Belongie, James Hays, Pietro Perona, Deva Ramanan, Piotr Dollár, and C Lawrence Zitnick. 2014. Microsoft coco: Common objects in context. In *Computer Vision–ECCV 2014: 13th European Conference, Zurich, Switzerland, September 6–12, 2014, Proceedings, Part V 13*. Springer, 740–755.
- [23] Chenxi Liu, Zhe Lin, Xiaohui Shen, Jimei Yang, Xin Lu, and Alan Yuille. 2017. Recurrent multimodal interaction for referring image segmentation. In *Proceedings of the IEEE international conference on computer vision*. 1271–1280.
- [24] Jihao Liu, Xin Huang, Yu Liu, and Hongsheng Li. 2022. Mixmim: Mixed and masked image modeling for efficient visual representation learning. *arXiv preprint arXiv:2205.13137* (2022).
- [25] Yinhan Liu, Myle Ott, Naman Goyal, Jingfei Du, Mandar Joshi, Danqi Chen, Omer Levy, Mike Lewis, Luke Zettlemoyer, and Veselin Stoyanov. 2019. Roberta: A robustly optimized bert pretraining approach. *arXiv preprint arXiv:1907.11692* (2019).
- [26] Gen Luo, Yiyi Zhou, Rongrong Ji, Xiaoshuai Sun, Jinsong Su, Chia-Wen Lin, and Qi Tian. 2020. Cascade grouped attention network for referring expression segmentation. In *Proceedings of the 28th ACM International Conference on Multimedia*. 1274–1282.
- [27] Gen Luo, Yiyi Zhou, Xiaoshuai Sun, Liujuan Cao, Chenglin Wu, Cheng Deng, and Rongrong Ji. 2020. Multi-task collaborative network for joint referring expression comprehension and segmentation. In *Proceedings of the IEEE/CVF Conference on computer vision and pattern recognition*. 10034–10043.
- [28] Xin Ma, Chang Liu, Chunyu Xie, Long Ye, Yafeng Deng, and Xiangyang Ji. 2022. Disjoint Masking with Joint Distillation for Efficient Masked Image Modeling. *arXiv preprint arXiv:2301.00230* (2022).
- [29] Edgar Margfroy-Tuay, Juan C Pérez, Emilio Botero, and Pablo Arbeláez. 2018. Dynamic multimodal instance segmentation guided by natural language queries. In *Proceedings of the European Conference on Computer Vision (ECCV)*. 630–645.
- [30] Varun K Nagaraja, Vlad I Morariu, and Larry S Davis. 2016. Modeling context between objects for referring expression understanding. In *Computer Vision–ECCV 2016: 14th European Conference, Amsterdam, The Netherlands, October 11–14, 2016, Proceedings, Part IV 14*. Springer, 792–807.
- [31] Adam Paszke, Sam Gross, Francisco Massa, Adam Lerer, James Bradbury, Gregory Chanan, Trevor Killeen, Zeming Lin, Natalia Gimelshein, Luca Antiga, et al. 2019. Pytorch: An imperative style, high-performance deep learning library. *Advances in neural information processing systems* 32 (2019).
- [32] Zhiliang Peng, Li Dong, Hangbo Bao, Qixiang Ye, and Furu Wei. 2022. Beit v2: Masked image modeling with vector-quantized visual tokenizers. *arXiv preprint arXiv:2208.06366* (2022).
- [33] Alec Radford, Jong Wook Kim, Chris Hallacy, Aditya Ramesh, Gabriel Goh, Sandhini Agarwal, Girish Sastry, Amanda Askell, Pamela Mishkin, Jack Clark, et al. 2021. Learning transferable visual models from natural language supervision. In *International conference on machine learning*. PMLR, 8748–8763.
- [34] Hengcan Shi, Hongliang Li, Fanman Meng, and Qingbo Wu. 2018. Key-word-aware network for referring expression image segmentation. In *Proceedings of the European Conference on Computer Vision (ECCV)*. 38–54.
- [35] Seungwoo Son, Namhoon Lee, and Jaeho Lee. 2023. MaskedKD: Efficient Distillation of Vision Transformers with Masked Images. *arXiv preprint arXiv:2302.10494* (2023).
- [36] Keyu Tian, Yi Jiang, Qishuai Diao, Chen Lin, Liwei Wang, and Zehuan Yuan. 2023. Designing BERT for Convolutional Networks: Sparse and Hierarchical Masked Modeling. *arXiv preprint arXiv:2301.03580* (2023).
- [37] Ashish Vaswani, Noam Shazeer, Niki Parmar, Jakob Uszkoreit, Llion Jones, Aidan N Gomez, Łukasz Kaiser, and Illia Polosukhin. 2017. Attention is all you need. *Advances in neural information processing systems* 30 (2017).
- [38] Zhaoqing Wang, Yu Lu, Qiang Li, Xunqiang Tao, Yandong Guo, Mingming Gong, and Tongliang Liu. 2022. Cris: Clip-driven referring image segmentation. In *Proceedings of the IEEE/CVF conference on computer vision and pattern recognition*. 11686–11695.
- [39] Jianzong Wu, Xiangtai Li, Xia Li, Henghui Ding, Yunhai Tong, and Dacheng Tao. 2022. Towards Robust Referring Image Segmentation. *arXiv preprint arXiv:2209.09554* (2022).
- [40] Zhenda Xie, Zheng Zhang, Yue Cao, Yutong Lin, Jianmin Bao, Zhuliang Yao, Qi Dai, and Han Hu. 2022. Simmim: A simple framework for masked image modeling. In *Proceedings of the IEEE/CVF Conference on Computer Vision and Pattern Recognition*. 9653–9663.
- [41] Zhendong Yang, Zhe Li, Mingqi Shao, Dachuan Shi, Zehuan Yuan, and Chun Yuan. 2022. Masked generative distillation. In *Computer Vision–ECCV 2022: 17th European Conference, Tel Aviv, Israel, October 23–27, 2022, Proceedings, Part XI*. Springer, 53–69.
- [42] Zhao Yang, Jiaqi Wang, Yansong Tang, Kai Chen, Hengshuang Zhao, and Philip HS Torr. 2022. Lavt: Language-aware vision transformer for referring image segmentation. In *Proceedings of the IEEE/CVF Conference on Computer Vision and Pattern Recognition*. 18155–18165.
- [43] Linwei Ye, Mrigank Rochan, Zhi Liu, and Yang Wang. 2019. Cross-modal self-attention network for referring image segmentation. In *Proceedings of the IEEE/CVF conference on computer vision and pattern recognition*. 10502–10511.
- [44] Licheng Yu, Zhe Lin, Xiaohui Shen, Jimei Yang, Xin Lu, Mohit Bansal, and Tamara L Berg. 2018. Mtnet: Modular attention network for referring expression comprehension. In *Proceedings of the IEEE conference on computer vision*

- and pattern recognition*. 1307–1315.
- [45] Licheng Yu, Patrick Poirson, Shan Yang, Alexander C Berg, and Tamara L Berg. 2016. Modeling context in referring expressions. In *Computer Vision–ECCV 2016: 14th European Conference, Amsterdam, The Netherlands, October 11–14, 2016, Proceedings, Part II* 14. Springer, 69–85.
- [46] Chaoyang Zhu, Yiyi Zhou, Yunhang Shen, Gen Luo, Xingjia Pan, Mingbao Lin, Chao Chen, Liujuan Cao, Xiaoshuai Sun, and Rongrong Ji. 2022. Seqtr: A simple yet universal network for visual grounding. In *Computer Vision–ECCV 2022: 17th European Conference, Tel Aviv, Israel, October 23–27, 2022, Proceedings, Part XXXV*. Springer, 598–615.